Chapter 4

Effects of Nearshore Upwelling on Coliform Dispersion near the Whites Point Outfall

David A. Siegel

Ocean Physics Group
Department of Geological Sciences
University of Southern California
Los Angeles, California

Burton H. Jones

Allan Hancock Foundation
University of Southern California
Los Angeles, California

Tommy D. Dickey

Ocean Physics Group
Department of Geological Sciences
University of Southern California
Los Angeles, California

Irwin Haydock

Los Angeles County Sanitation Districts
Whittier, California

Alan Bratkovich

Ocean Physics Group
Department of Geological Sciences
University of Southern California
Los Angeles, California

ABSTRACT

The relationships between nearshore physical processes and outfall effluent distributions were studied during the period 5 May to 15 June 1982 at the Whites Point outfall of the Los Angeles County Sanitation Districts (California, U.S.A.). Physical parameters were sampled from a mooring located near the end of one of the two outfall diffusers (~2.5 km offshore, 60-m depth). Moored instrumentation included a wind anemometer, vector-measuring current meters at 7- and 44-m depths, and 18 thermistors spaced uniformly throughout the water column. Total coliform bacterial counts were sampled at nearby beach stations. During the 40-d period, two cooling (upwelling) events and one warming (relaxation) event were observed. The upwelling episodes were characterized by southeastward longshore winds of from 3 to ~5 m s^{-1}, offshore surface flow, near-surface water temperatures of 14°C or less, and cooling rates of ~1°C d^{-1}. A cessation of the upwelling response was induced by a weak northwestward wind event. The relaxation response was strongest in the longshore current field, which showed an energetic northwestward pulse of several days' duration. The associated temperature response was strongest near the surface (the total increase in temperature was ~2°C). The beach coliform bacterial counts generally increased during the upwelling and decreased during the non-upwelling events. Evidence is presented that supports the hypothesis that upwelling was the major process contributing to transport of bottom-discharged effluent toward the beaches during this observational period.

4.1. INTRODUCTION

Oceanic wastewater outfall flows may be characterized as turbulent buoyant plumes. Koh and Brooks (1975) described three stages in the dispersal of a turbulent buoyant plume into a stratified fluid: (1) the plume rises and entrains the ambient fluid until the buoyancy of the effluent stream has been dissipated; (2) the plume spreads horizontally along its newly found constant density surface; and (3) the effluent becomes dynamically passive and is advected by the far-field flow.

The time scales of the mixing and advective processes relative to the lifetime of the pollutant give some estimate of the suitability of using an ocean outfall for the disposal of a pollutant. Koh and Brooks (1975) concluded that the first two stages of dispersion generally occur on time scales of <3 h. Since coliform bacteria in seawater have lifetimes on the order of several days (Chamberlain and Mitchell, 1978), most of the lifetime of these bacteria is spent being advected and mixed by the ambient physical oceanographic processes. In other words, the third step (listed above) of the conceptual dispersal process is of primary importance in determining the ultimate dispersion of water-borne wastes. The objective here is to illustrate how these far-field processes contribute to the dispersal of a wastewater effluent plume, using the Whites Point ocean outfall near Los Angeles, California, as a case study.

Nearshore upwelling is the primary far-field oceanographic dispersive process examined in this chapter. Nearshore upwelling has been described by many authors [see Brink (1983) for a review] and is commonly observed along the California coast (Sverdrup, 1938; Huyer, 1983; Jones et al., 1983) where upwelling is characterized by longshore southward winds creating offshore Ekman transport in the surface layers. Conservation of mass requires that the near-surface waters be replaced by denser (colder) waters that are advected from depth. The wind-induced vertical velocity in the subsurface region is referred to as the upwelling velocity. The onshore flow of denser (colder) water caused by the offshore surface transport also leads to upward sloping (as the coastline is approached), isopycnal (isothermal) surfaces. It is hypothesized that, because of the wind-driven upwelling, the subsurface effluent stream is advected preferentially toward the coast. It will be demonstrated that the dynamics of the system are dominated by wind-driven upwelling, and further, that the concentrations of effluent observed at beach locations correlate well with upwelling-dominated flows.

4.2. EXPERIMENTAL METHODS

The Whites Point outfall of the Los Angeles County Sanitation Districts (LACSD) is located on the south side of the Palos Verdes Peninsula near Los Angeles, California (Fig. 4.1). The outfall terminates in 60 m of water, and ~30% of its length is the diffuser; hence, the source of the effluent cannot be described as a point source. The LACSD installed a physical oceanographic buoy with a surface float near the end of the outfall. The buoy instrumentation included 18 thermistors with a vertical spacing of ~3 m (one failed). The LACSD also deployed two vector-measuring current meters (VMCMs) located at 7- and 44-m depths and a wind anemometer located 3 m above the mean sea surface. The data were transmitted by telemetry to shore every 30 min. Forty days (5 May 1982 through 15 June 1982 or Julian days 125–165) of the entire record had complete enough data (nearly continuous) for thorough analysis. Subinertial variance ellipses (similar to

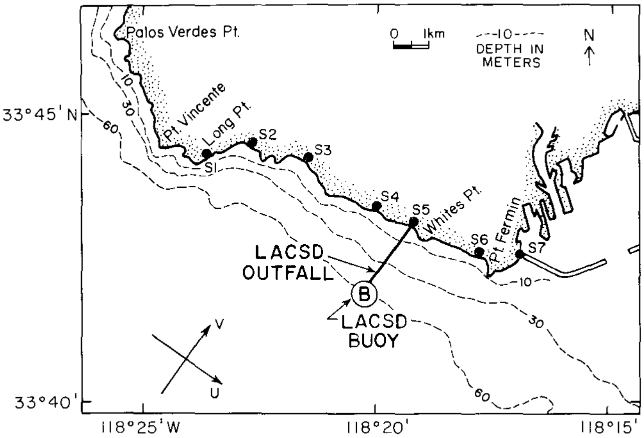

Figure 4.1. Geometry and bathymetry of the Whites Point outfall region. S1–S7 refer to the beach collection stations. The *U* and *V* axes refer to the coordinate system used in this analysis. Dashed lines indicate depth in meters.

tidal ellipses) indicated a directional ambiguity (±90°) in the data recorded by the bottom (44-m) VMCM. Hence, these data were of limited utility for the analysis.

A coordinate system was established (Fig. 4.1) to describe the longshore and onshore components of horizontal velocity. The *U* component of velocity is defined to be longshore with the positive direction pointed approximately toward the southeast, and the *V* component is defined to be in the cross-shelf direction with positive onshore or approximately toward the northeast. Previous work indicates that this region may be characterized by subsurface cross-shelf flows at subinertial frequencies (Stevenson and Gorsline, 1956; Whitledge and Bishop, 1972). The local bathymetry is generally parallel to the coast with a cross-shelf slope of ~0.03 (30 m km^{-1}).

Total coliform bacterial counts were monitored at seven beach stations (Fig. 4.1, S1–S7) as part of the LACSD monitoring program. The beach stations spanned 12 km of coastline and were sampled daily at ~1000 Pacific Standard Time. Bacterial counts were determined by using a standard filtration technique. The coliform bacterial counts were logarithmically transformed ($\log_{10}(n + 1)$) and then smoothed by a 3-point (3-d) running mean. Buoy data were averaged by using 12-h bins and smoothed with a 5-point (2.5-d) running mean. These procedures were used to remove variability associated with surface tides, internal gravity waves, surface waves, internal tides, and diurnal sea breeze effects. Thus, frequencies between 0.05 cycle d^{-1} and 0.4 cycle d^{-1} were analyzed. The time scale of this frequency band is often termed the synoptic scale (Jones et al., 1983). Additional data from an LACSD hydrographic survey cruise were also used.

4.3. RESULTS

A cross-shelf temperature section (day 148, or 28 May) indicated relatively cool water nearshore with no surface mixed layer (Fig. 4.2). A general characteristic of the vertical temperature profile was an intense thermocline seen in the upper 30 m. The vertical temperature gradient in the thermocline was ~0.2°C m^{-1}. The isotherms generally sloped upward toward the beach; the slope of the 13°C isotherm was ~3 m km^{-1}. This suggests that upwelling was occurring during this survey.

The buoy measurements provide time series of wind speed and direction, horizontal currents at 7 m, and temperature at 17 depths (Fig. 4.3a,b,c). The interrelationships among these variables will be examined in the context of a wind-forced upwelling event.

The winds (Fig. 4.3a) were predominantly downcoast (trending toward the southeast) with the exception of the period from day 136 to 140. These prevailing (longshore) winds are considered to be favorable for upwelling (i.e., capable of producing offshore Ekman transport in the near-

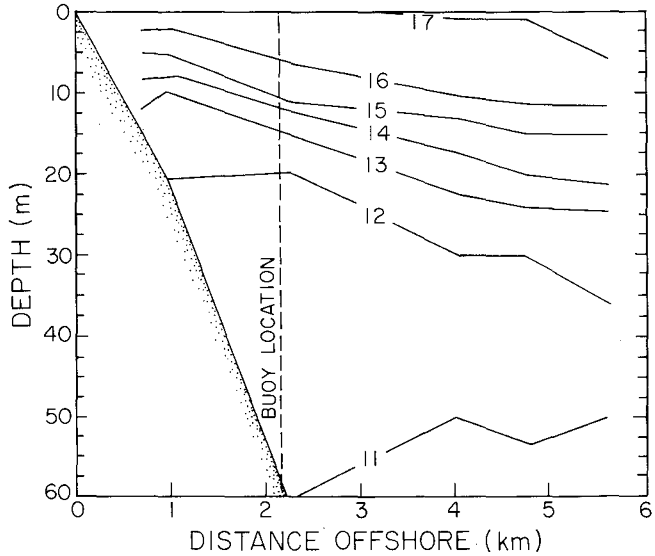

Figure 4.2. Cross-shelf temperature section (°C) from a LACSD hydrographic survey on 28 May 1982. The dashed line indicates the buoy location.

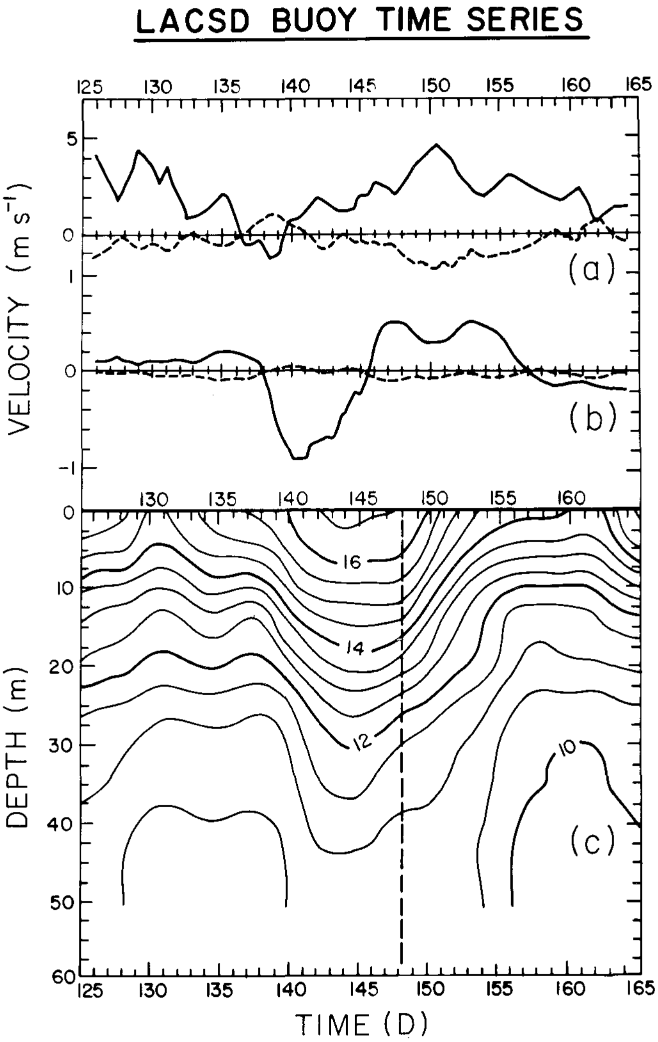

Figure 4.3. The 40-d time series of the low-pass buoy records of (a) winds, (b) horizontal currents at 7-m depth, and (c) vertical temperature profile. For (a) and (b) the units are m s^{-1}, the solid lines are the U component (downcoast), and the dashed lines are the V component (onshore). For (c) the units are °C.

surface layer). The two periods of upwelling-favorable winds (prior to day 136 and after day 140) were separated by a 4-d wind-reversal episode when the wind was onshore and upcoast. The maximum upwelling-favorable winds (>3 m s^{-1}) occurred between days 125 and 132 and between days 148 and 156. The unsmoothed wind data indicate a large diurnal sea breeze component, which will not be discussed in this chapter.

The temporal evolution of the subsurface temperature structure (Fig. 4.3c) is the primary indicator of upwelling. The most obvious features are the warming event (between days 138 and 144) and the cooling event (between days 144 and 156). During the warming event, the temperature increased ~2°C in the upper layer, but during the cooling event it decreased ~3°C. The upwelling velocity during the cooling event is estimated from isotherm displacements to be ~3.5 m d^{-1}. The temperature record also indicated a net cooling at depth (i.e., the 12°C isotherm rose ~10 m). Similar observations of nearshore cooling at depth during the spring and summer seasons have been reported by Winant and Bratkovich (1981) off Del Mar, California. This effect is consistent with onshelf transport of cooler deep water (i.e., upwelling). The unsmoothed temperature record from the buoy showed a high degree of variability at semi-diurnal frequencies. The isotherm displacement associated with these motions was 5–10 m. These large near-tidal motions will obviously contribute to the variability of a tracer (i.e., the coliform bacteria) observed in the natural system.

Winds favorable to upwelling were associated with decreasing water temperatures. The wind reversal appears to be well correlated (at a 2-d lag) with the warming event observed in the buoy temperature record. As seen in the measured isotherm displacements (about day 144–156), upwelling returned ~4–5 d after the start of wind intensification (on about day 140). The warming event represents the relaxation portion of the upwelling event cycle. This episodic upwelling cycle is common to the California coast and has a typical period of 3–10 d (Huyer, 1983).

Data from the upper VMCM (7-m depth) indicate downcoast, slightly offshore flow approximately coincident with (though lagging) upwelling-favorable winds (Fig. 4.3b). The upper-ocean response to upwelling-favorable winds described here is generally consistent with the classical description of nearshore upwelling (e.g., Brink, 1983). On day 138 (the onset of extreme warming), an intense upcoast and slightly onshore flow was indicated by the upper VMCM record. This flow coincided with the relaxation of the upwelling (onset of warming) observed in the temperature record but again lagged the wind by about 2 d. The flow direction reversed on day 145 and again returned to the upwelling state. This flow reversal lagged the wind reversal but was nearly coincident with the apparent onset of ascending isotherms. Due to the relative weakness of the surface wind forcing, several processes may be associated with coastal cooling (such as longshore advection), which may account for the relatively large time lag observed. The maximum upwelling-favorable currents correlate reasonably well (after phase shifting) with the maximum upwelling-favorable winds.

The beach coliform bacterial count (*C*) time series is shown in Fig. 4.4. Large inter-station variability was obvious; however, the overall station average showed several distinct periods. Periods of higher counts ($\log_{10} C > 1$) were noted for days 126–131 and 155–164; and periods of lower counts ($\log_{10} C < 0.5$) for days 133–140 and 147–154. In a qualitative sense, the periods with high bacterial counts coincided with upwelling (cooling), and the periods with low bacterial counts were associated with the warming trend (up to about day 140). However, this simple relationship, based upon ocean temperature alone, is invalid for days 140–147. This particular episode lags the only period of onshore–upcoast surface flow by ~2 d. One may speculate that the high coliform bacterial counts are associated with the surface onshore flow of the buoyant organic component of the effluent stream (Word et al., 1986). Unfortunately, based upon these data, a conclusive statement cannot be made. A major transition in the average coliform counts was observed on day 154. This transition is nearly coincident with the most pronounced upwelling as observed from the buoy measurements.

4.4. DISCUSSION AND CONCLUSIONS

The use of coliform bacteria as tracers of effluent dispersion has several obvious problems. First, the concentration of coliform bacteria is not a simple function of mixing and advection. Coliform bacterial growth and decay rates are functions of variables such as temperature, nutrients, dissolved organic carbon, solar radiation (particularly ultraviolet), and predation. These variables change by several orders of magnitude in a nearshore environment, especially in the vicinity of a wastewater outfall. Furthermore, the determination of coliform bacterial counts is subject to measurement errors, and standard deviations of measured values are, at times, of the same order as the mean values.

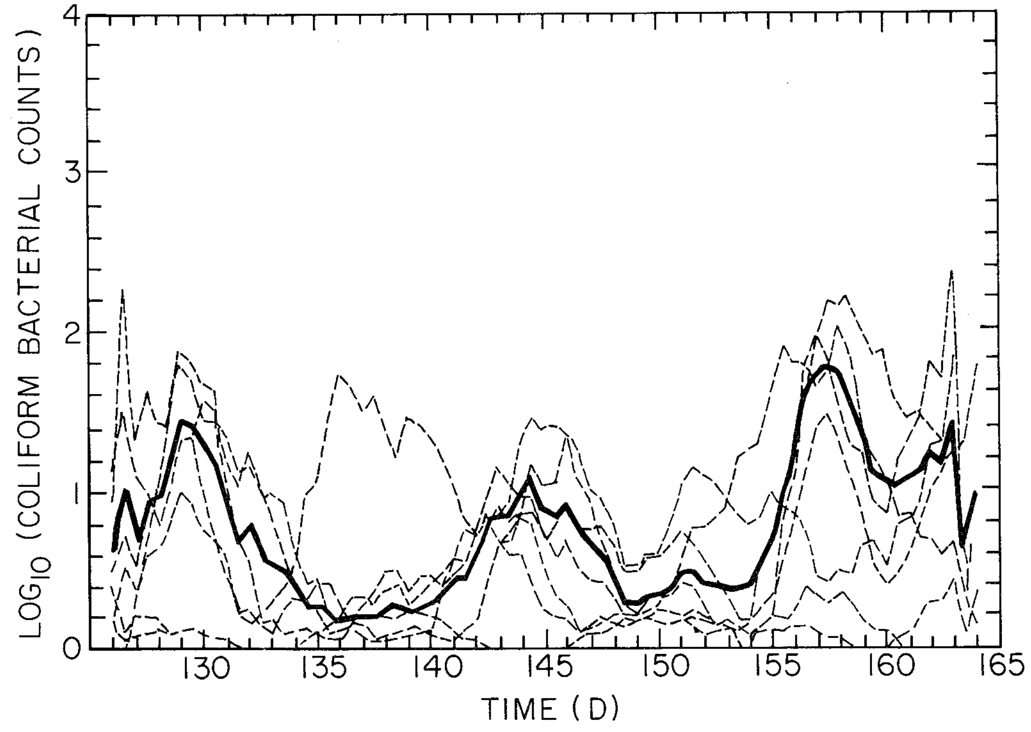

Figure 4.4. Time series of total coliform bacterial counts. Units are $\log_{10}$ (counts per 100 ml + 1). The heavy line is the average of the seven station values shown.

Other factors also contribute to the variability of the results. The shoreline and local bathymetry are irregular, and, as mentioned earlier, the diffuser is a non-uniform line source rather than a point source of effluent. These irregularities in coastal and diffuser geometries make models of effluent advection difficult to construct and interpret. The effects both of tidal and of solar cycles could also contribute to the sample variability. Despite these difficulties, there is reasonable evidence that upwelling was a major process contributing to beachward transport of effluent. Wind-driven upwelling was observed at the LACSD Whites Point wastewater outfall during May and June 1982. The average coliform bacterial counts appear to be generally well correlated with these upwelling events.

ACKNOWLEDGMENTS

This project was funded by the Los Angeles County Sanitation Districts. Support for this work was also obtained from the University of Southern California–Sea Grant Program. D. Siegel would also like to acknowledge support from the Graduate Research Fellowship Program of the Office of Naval Research, administered by American Society for Engineering Education. Discussions with Gary Kleppel and Rodolfo Iturriaga were most useful. Hermawan Indrapradja and Edward Hurst assisted with the preliminary data analysis. Sue Turnbow expeditiously typed the manuscript and Janet Dodds expertly drafted the figures.

REFERENCES

Brink, K. H. 1983. The near surface dynamics of coastal upwelling. *Progress in Oceanography*, **12**, 233–257.

Chamberlain, C. E., and R. Mitchell. 1978. A decay model for enteric bacteria in natural waters. *In*: Water Pollution Microbiology, Vol 2, R. Mitchell (Ed.). John Wiley and Sons, New York, pp. 325–348.

Huyer, A. 1983. Coastal upwelling in the California current system. *Progress in Oceanography*, **12**, 259–284.

Jones, B. H., K. H. Brink, R. C. Dugdale, D. W. Stuart, J. C. Van Leer, D. Blasco, and J. C. Kelley. 1983. Observations of a persistent upwelling center off Point Conception, California. *In*: Coastal Upwelling Part A, E. Suess and J. Thiede (Eds.). Plenum Press, New York, pp. 37–60.

Koh, R. C. Y., and N. H. Brooks. 1975. Fluid mechanics of waste-water disposal in the ocean. *Annual Review of Fluid Mechanics*, **7**, 187–211.

Stevenson, R. E., and D. S. Gorsline. 1956. A shoreward movement of cool subsurface water. *Transactions of the American Geophysical Union*, **32**, 180–184.

Sverdrup, H. V. 1938. On the process of upwelling. *Journal of Marine Research*, **2**, 155–164.

Whitledge, T. E., and D. Bishop. 1972. Data Report: *R/V T. G. Thompson* Cruise 67 (MESCAL I-OUTFALL I), Part II: Outfall I, Hydrography and Productivity. Special Report 51, University of Washington, Seattle, 391 pp.

Winant, C. D., and A. W. Bratkovich. 1981. Temperature and currents of the Southern California shelf: a description of the variability. *Journal of Physical Oceanography*, **11**, 71–86.

Word, J. Q., C. D. Boatman, C. C. Ebbesmeyer, R. E. Singer, S. Fischnaller, and Q. J. Stober. In press. Vertical transport of freon extractable and non-extractable material and bacteria (fecal coliforms and Enterococci) to the surface of marine waters: some experimental results using secondary sewage effluent. *In*: Oceanic Processes in Marine Pollution, Vol. 6: Physical and Chemical Transport and Transformation, D. Baumgartner and I. W. Duedall (Eds.). R. E. Krieger Publishing Company, Malabar, Florida, in press.